

MIT Open Access Articles

Roughness-Induced Pavement-Vehicle Interactions

The MIT Faculty has made this article openly available. **Please share** how this access benefits you. Your story matters.

Citation: Louhghalam, Arghavan, et al. "Roughness-Induced Pavement-Vehicle Interactions: Key Parameters and Impact on Vehicle Fuel Consumption." *Transportation Research Record: Journal of the Transportation Research Board*, vol. 2525, Jan. 2015, pp. 62-70.

As Published: <http://dx.doi.org/10.3141/2525-07>

Publisher: SAGE Publications

Persistent URL: <http://hdl.handle.net/1721.1/117498>

Version: Original manuscript: author's manuscript prior to formal peer review

Terms of use: Creative Commons Attribution-Noncommercial-Share Alike



1 **ROUGHNESS-INDUCED PAVEMENT-VEHICLE INTERACTIONS: KEY PARAMETERS AND IMPACT**
2 **ON VEHICLE FUEL CONSUMPTION**

3 By: A. Louhghalam¹, M. Akbarian², F.-J. Ulm³

4 Submission Date: July 30, 2014

5 Word Count: 4244 + 9 Figures + 3 Tables = 7244

6 Affiliation/Address:

7 ¹Arghavan Louhghalam,
8 Department of Civil & Environmental Engineering
9 Massachusetts Institute of Technology
10 Cambridge MA 02139
11 Email: arghavan@mit.edu

12 ²Mehdi Akbarian
13 Department of Civil & Environmental Engineering
14 Massachusetts Institute of Technology
15 Cambridge MA 02139
16 Email: akbarian@mit.edu

17 ³Franz-Josef Ulm (Corresponding Author)
18 Department of Civil & Environmental Engineering
19 Massachusetts Institute of Technology
20 Bldg. 1-263
21 77 Massachusetts Avenue
22 Cambridge MA 02139
23 Tel: 617-253.3544
24 Emails: ulm@mit.edu

25
26

1 **Abstract:** Pavement roughness affects rolling resistance, and thus vehicle fuel consumption. In fact,
2 when a vehicle travels at constant speed on an uneven road surface, the mechanical work dissipated in
3 the vehicle's suspension system is compensated by vehicle engine power, resulting in excess fuel
4 consumption. This dissipation depends on both road roughness and vehicle dynamic characteristics.
5 Herein we propose, calibrate and implement a mechanistic model for roughness-induced dissipation.
6 The distinguished feature of our model is that it combines a thermodynamic quantity (energy
7 dissipation) with results from random vibration theory in order to identify the governing parameters
8 that drive the excess fuel consumption due to pavement roughness; namely the international Roughness
9 Index (IRI) and the waviness number, w (a Power Spectral Density parameter). It is shown via sensitivity
10 analysis that the sensitivity of model output, i.e. the excess fuel consumption, to the waviness number is
11 significant and comparable to that of IRI. Thus, introducing the waviness number as a second roughness
12 index, in addition to IRI, allows a more accurate quantification of the impact of surface characteristics on
13 vehicle fuel consumption and the corresponding greenhouse gas emission. This is illustrated by an
14 application of our roughness-fuel consumption model to two road profiles extracted from FHWA's Long
15 Term Pavement Performance (LTPP) database.

1 INTRODUCTION

2 It has long been recognized that pavement roughness affects the pavement vehicle interaction (PVI),
 3 and contributes to the vehicle operating costs (VOC) (1,2). The most prominent VOC model is the HDM4
 4 model which relates a measurable pavement roughness parameter, the International Roughness Index
 5 (IRI) introduced originally for quantifying ride comfort (3,4), through empirically calibrated vehicle-
 6 dependent functional relations, to fuel consumption (5,6). Such VOC models have recently gained some
 7 new importance within the context of engineering life-cycle-assessment (LCA) methods of pavement
 8 structures that relate pavement condition to rolling resistance and corresponding fuel consumption and
 9 environmental impacts (7). This background provides motivation for this study that aims at identifying
 10 the key parameters for roughness-induced fuel consumption.

11 More specifically, roughness-induced fuel consumption is due to energy dissipation in vehicle's
 12 suspension system: when a vehicle travels at constant speed on an uneven road surface, the mechanical
 13 work dissipated in the vehicle's suspension system is compensated by additional vehicle engine power.
 14 Thus, a mechanistic model of the actual energy dissipation is expected to provide a direct means to
 15 relate pavement roughness and vehicle-specific physical quantities to fuel consumption. This is shown in
 16 the first part of this paper. Instead of using a single value roughness index, such as IRI, we employ the
 17 roughness power spectral density (PSD) as a refined means to describe the distribution of roughness
 18 across various wavelengths. We then show how this mechanistic model can be calibrated when using
 19 the HDM4-model. Finally, by way of application, the novel VOC model is employed using road profiles
 20 extracted from FHWA's Long Term Pavement Performance (LTPP) database, and the difference between
 21 our prediction and the HDM4 model in terms of dissipation and fuel consumption is discussed.

22

23 THEORETICAL BACKGROUND: MECHANISTIC MODEL FOR ROUGHNESS-INDUCED PVI

24 For a first-order evaluation of the energy dissipation by a vehicle's suspension system, we consider the
 25 classical two-degree-of-freedom (2-DOF) quarter-car model (8) (Figure 1(a)): a two-mass system in series
 26 composed of a tire (stiffness k_t) and a spring-dashpot parallel suspension unit (stiffness k_s and viscosity
 27 coefficient C_s). The dissipation of mechanical work into heat form is only due to the relative motion,
 28 $\dot{z} = dz/dt$ (with z the relative displacement of sprung mass m_s with respect to the unsprung mass m_u)
 29 of the suspension system, i.e. $\delta D = C_s \dot{z}^2$; or when expressed in terms of the expected value of energy
 30 dissipated per traveled length at constant speed V :

$$31 \quad E[\delta \mathcal{E}] = \frac{C_s}{V} E[\dot{z}^2] \quad (1)$$

32 The suspension motion $\dot{z} = dz/dt$ is due to road roughness transmitted from the ground via tire
 33 stiffness k_t . It is generally assumed that road roughness ξ is a zero-mean stationary Gaussian process
 34 (9). In practice the power spectral density of road profile is represented as a power function of the
 35 angular wavenumber, Ω (10):

$$36 \quad S_\xi(\Omega) = c|\Omega|^{-w} \quad (2)$$

37 where the unevenness index, c , and the waviness number, w , characterize the road profile. In fact, Eq.
 38 (2) is a linear function in logarithmic space with slope w for which the larger values indicate the
 39 presence of longer wavelengths. The use of a PSD representation allows the employment of random
 40 vibration theory to link the mean square of suspension motion in Eq. (1) to both dynamic properties of
 41 the vehicle and roughness parameters (11):

$$1 \quad E[\dot{z}^2] = \int_0^\infty V^2 \Omega^2 |H_s(V\Omega)|^2 S_\xi(\Omega) d\Omega \quad (3)$$

2 where $H_s(\omega)$ is the dimensionless frequency response function (FRS) that relates the relative
3 suspension deformation to the road roughness profile:

$$4 \quad H_s(\omega) = \frac{\omega^2 k_t m_s}{(-m_u \omega^2 + i C_s \omega + k_t + k_s)(-m_s \omega^2 + i C_s \omega + k_s) - (i C_s \omega + k_s)^2} \quad (4)$$

5 with $\omega = V\Omega$ the angular frequency. The above FRS depends only on dynamic properties of vehicle
6 (quarter-car in case of simple 2-DOF model) while roughness PSD carries the information on pavement
7 surface characteristics.

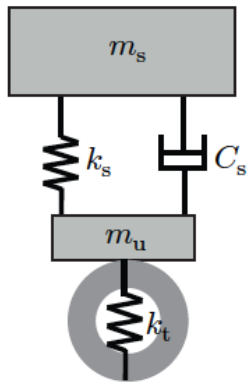
8 Thus, combining equations (1) and (3), the expected value of dissipated energy per unit length
9 traveled is obtained in a form that relates the dissipated energy in the car suspension to road surface
10 properties via roughness PSD parameters (i.e. waviness number w and the unevenness index c) as well
11 as vehicle properties via FRS:

$$12 \quad E[\delta\mathcal{E}] = c C_s V \int_0^\infty \Omega^{2-w} |H_s(V\Omega)|^2 d\Omega \quad (5)$$

13 Or, in terms of the circular frequency:

$$14 \quad E[\delta\mathcal{E}] = c C_s V^{w-2} \int_0^\infty \omega^{2-w} |H_s(\omega)|^2 d\omega \quad (6)$$

15 Recognizing that the argument inside the integral of Eq. (6) does not depend on vehicle speed, the
16 energy dissipation is found to scale with the vehicle speed as $E[\delta\mathcal{E}] \sim V^{w-2}$. That is, for waviness
17 numbers, $w > 2$, the roughness-induced dissipated energy increases with the speed, and for $w < 2$ it is
18 the inverse. We keep this scaling in mind for later applications.



(a)

Property	value
k_t/m_s [s^{-2}]	653
k_s/m_s [s^{-2}]	63.3
C_s/m_s [s^{-1}]	6.0
m_u/m_s [1]	0.15

(b)

19

20 **FIGURE 1 (a): 2-DOF Quarter-car model; (b): dynamic properties of the golden-car used for evaluation**
21 **of IRI.**

22

23 At this stage of the development, it is appropriate to close the loop with other roughness-
24 induced VOC models based on the International Roughness Index (IRI), such as the HDM4-model (5,6)

1 for vehicle fuel consumption and related GHG emissions. To this end, we remind us that IRI is defined as
 2 the average rectified velocity of a specific quarter-car (golden-car) traveling at $V_0 = 22.2$ m/s (80 km/h):

$$3 \quad \text{IRI} = \frac{1000}{V_0 L} \int_0^L |\dot{z}_{GC}| dx \quad (7)$$

4 where the subscript GC denotes the golden-car properties, given in Figure 1(b). Assuming the road
 5 profiles are stationary Gaussian processes, the expected value of IRI can be written in terms of
 6 roughness PSD parameters in the form (11):

$$7 \quad E[\text{IRI}] = \sqrt{\frac{2}{\pi} V_0^{w-3} c \int_0^\infty \omega^{2-w} |H_{s-GC}(\omega)|^2 d\omega} \quad (8)$$

8 where H_{s-GC} is the FRS of the Golden Car. A final substitution of Eq. (8) into Eq. (6) provides the
 9 following expression for the energy dissipation:

$$10 \quad E[\delta\mathcal{E}] = \frac{\pi}{2} C_s V_0 \times \left(\frac{V}{V_0}\right)^{w-2} \times \frac{\int_0^\infty \omega^{2-w} |H_s(\omega)|^2 d\omega}{\int_0^\infty \omega^{2-w} |H_{s-GC}(\omega)|^2 d\omega} \times E[\text{IRI}]^2 \quad (9)$$

11 Expression (9) is of particular interest in order to fully appreciate the added value of the mechanistic-
 12 based roughness-induced PVI model compared to other empirical models. Specifically, the dissipated
 13 energy scales with the square of (the expected value) of IRI; and also depends on the waviness number,
 14 w . Hence, a calibration of the model requires consideration of (at least) a second pavement roughness
 15 parameter, in addition to IRI. This is shown here below.

16

17 CALIBRATION WITH HDM4 MODEL

18 The mechanistic roughness-induced PVI model in expression (9) relates surface characteristics to
 19 roughness-induced energy dissipation and the resulting excess fuel consumption by using a simple 2-
 20 DOF system as a quarter-vehicle model. In reality the dynamic behavior of vehicles is far more
 21 complicated to be comprehensively captured by a single quarter-car model. While inertial properties
 22 (such as sprung and unsprung masses) of the vehicle can be estimated with reasonable accuracy, the
 23 stiffness properties are not easy to evaluate; since the total stiffness involved in different components of
 24 a vehicle is more complex than the stiffness of suspension and tire.

25 As an alternative, and in the absence of such detailed measurements, we use the HDM4 model
 26 (5,6) to calibrate our mechanistic roughness-induced PVI model. Such a calibration aims at determining
 27 the stiffness properties for the different vehicle classes, together with the road waviness number as an
 28 additional adjustable parameter. In the HDM4 model the variation of excess fuel consumption due to a
 29 unit change in IRI is reported for different driving speeds and for five vehicle classes: medium car, SUV,
 30 Van, light truck and articulated truck. The properties of these vehicles, obtained from literature are
 31 summarized in Table 1. To calibrate the model, we use total fuel consumption evaluated from HDM4
 32 model at reference $\text{IRI}_0 = 1\text{m/km}$ as baseline, $\text{IFC}_0 = \text{IFC}(\text{IRI}_0)$, and convert roughness-induced
 33 dissipated energy evaluated from equation (9) to excess fuel consumption using an engine efficiency
 34 coefficient (ξ_b in mL/kW/s, given for the vehicle classes in Table 1):

$$35 \quad E[\delta\text{IFC}] = \xi_b E[\delta\mathcal{E}] \quad (10)$$

1 The percent change in fuel consumption due to change in IRI relative to reference IRI₀ using the
2 mechanistic model is thus evaluated:

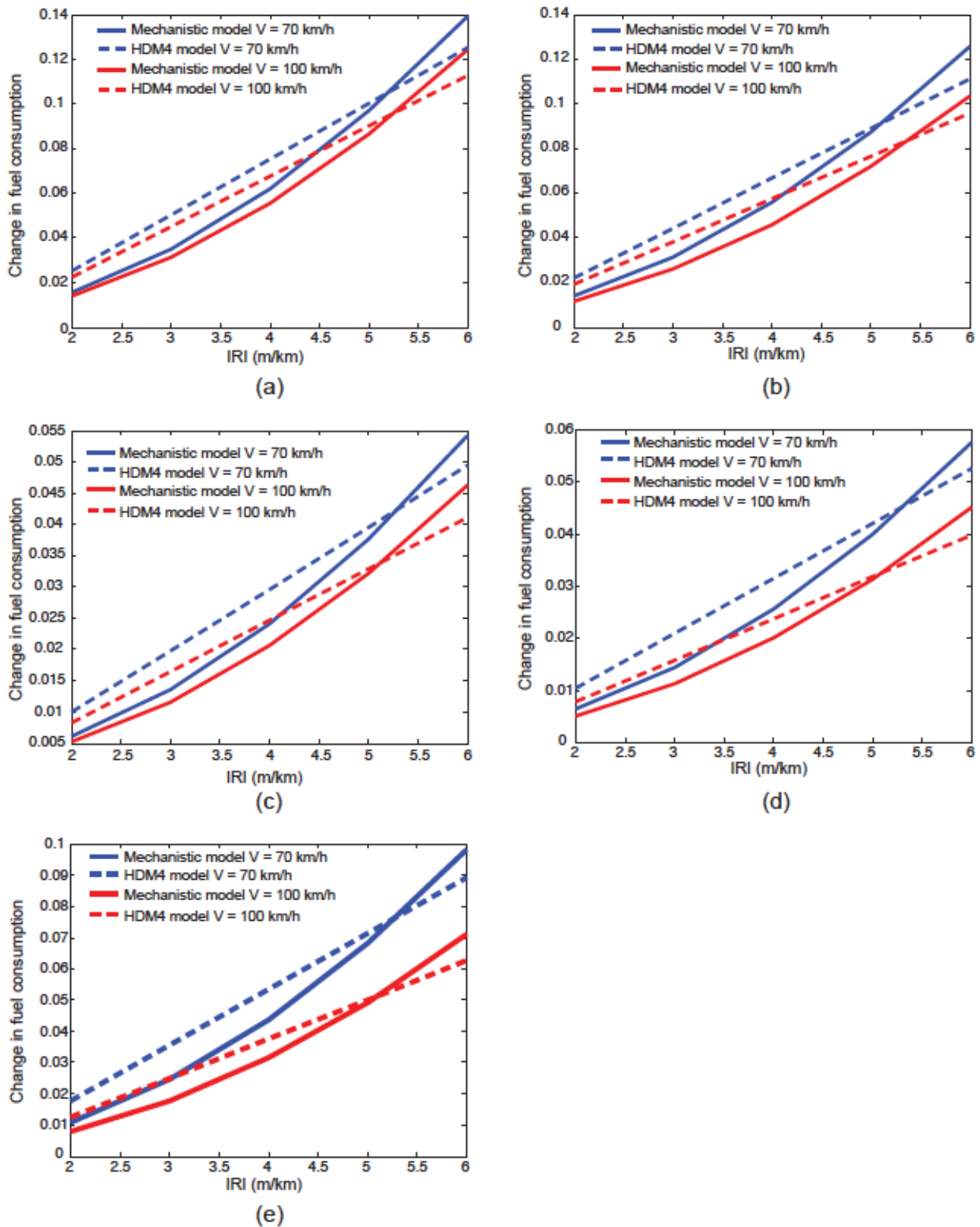
$$3 \frac{E[\delta IFC(IRI)] - E[\delta IFC(IRI_0)]}{IFC_0} \times 100 \quad (11)$$

4 The corresponding data points $IFC(IRI, V)/IFC_0 - 1$ from calibrated HDM4 model is also obtained for
5 IRI values varying from 1 to 6 m/km and vehicle speeds 56-112 km/h associated with the range of
6 vehicle speed in field measurements (5). Model calibration is performed by minimizing the difference
7 between the predicted change in excess fuel consumption from the two methods by adjusting a single
8 value for waviness number w and five dimensionless stiffness-mass coefficients $\beta_j = \sqrt{k_t m_s / (k_s m_u)}$
9 for each vehicle class. The results of the optimization procedure are illustrated, for the five vehicle
10 classes, in Figure 2 for two vehicle speeds, 70 and 100 km/h, in form of plots of the total fuel
11 consumption vs. IRI, comparing our results with the predictions of the HDM4 model (5). Unlike the
12 HDM4 model that relates the excess fuel consumption linearly to IRI, the mechanistic model presented
13 here establishes a functional relationship between the excess fuel consumption and the square of IRI,
14 observed both in Eq. (9) and Figure 2. The fitted dimensionless coefficients β_j are summarized in Table
15 1. Furthermore, the waviness number obtained in the optimization procedure is $w = 2.4117$, which
16 agrees well with the probability distribution of waviness number w of the Long-Term Pavement
17 Performance (LTPP) program of the US Federal Highway Administration (FHWA) reported by Kropac and
18 Mucka (12), which exhibits a mode at around $w = 2.5$. We consider this agreement as an independent
19 validation of our modeling approach of roughness-induced PVI.

20 **TABLE 1 Vehicle Dynamical Properties Given per Axel. (❖ : CarSim Template, ♦ :GMC Specification**
21 **Manual)**

Car class Properties	Medium Car	SUV	VAN	Light Truck	Articulated Truck
m_t (ton)	1.46 (4)	2.5 (4)	2.54 (4)	6.5 (4)	34.9 (4)
m_s (kg)	80 (19)	125 ❖	134 (20)	395 ♦	544 (21)
k_s (KN/m)	29.44 (19)	189 ❖	48	337 ♦	700 (21)
ξ_b	.096 (4)	.072 (4)	.072 (4)	.062 (4)	.059 (4)
β	46.98	28.03	31.00	14.90	13.30

22



1

2 **FIGURE 2** Roughness-induced change in fuel consumption in function of IRI at V=70 and 100 km/h for
 3 (a): medium car; (b): SUV; (c): van; (d): light truck and (e): articulate truck.

4

1 SENSITIVITY ANALYSIS

2 To complete this investigation of roughness-induced PVI, it is instructive to investigate the
3 sensitivity of the model-based estimated excess fuel consumption w.r.t. the uncertainty in model input
4 parameters. Such a sensitivity analysis aims at identifying the main factors driving the uncertainty of
5 model output and quantifies the associated contribution. Herein, we use the Spearman rank correlation
6 coefficient (SRCC) (13) to determine the sensitivity of the energy dissipation to input parameters of the
7 roughness model. The SRCC method falls under the large category of global sensitivity analysis, which –
8 in contrast to local sensitivity analysis – provides information about the sensitivity of the model output
9 to all input variables across the entire design space and accounts for the interaction between different
10 input parameters. To this end, we perform Monte-Carlo simulations by generating realizations of input
11 parameters according to their distribution in the roadway network. Using the roughness mechanistic
12 model in equation (9) for each realization we evaluate roughness-induced dissipation and relevant fuel
13 consumption. We then use this result to evaluate SRCC between each input parameter and the excess
14 fuel consumption.

15 Monte-Carlo Simulation

16 The calibrated roughness-induced dissipation model in Eq. (9) is characterized by three independent
17 inputs parameters: IRI, waviness number (w) and vehicle speed (V). To perform Monte-Carlo simulation
18 these input parameters must be generated according to their probability density functions (PDFs).

19 For the distribution of IRI and waviness number, we use the results of the empirical distributions
20 of the LTPP program of the US FHWA dataset reported by Kropac and Mucka (12). As shown in Figure 3,
21 the PDFs of both IRI and waviness number follow respectively a lognormal and a truncated normal
22 distribution with mean and standard deviation summarized in Table 2. The probability density function
23 for vehicle speed is evaluated from the Highway Fuel Economy Driving Schedule (HWFED) provided by
24 the US Environmental Protection Agency (EPA), which represents highway driving conditions for vehicles
25 traveling under 60 mph (14). Since our model is developed under the steady state assumption for
26 constant vehicle speed, the vehicle speeds associated with stop and go condition, i.e. speeds lower than
27 30mph at the beginning and end of speed time history, are filtered out for PDF estimation (see Figure 4).

28 To generate a random number with cumulative distribution function (CDF) $F_X(x)$ we use the
29 inverse transformation technique: first a random variable U with uniform distribution $U \sim u[0,1]$ is
30 generated. It can be readily shown that the inverse of the cumulative distribution function evaluated at
31 U , $X = F_X^{-1}(U)$, is a random variable with CDF $F_X(x)$. The technique is used here to generate random
32 variables from parametric distributions shown in Figure 3 (lognormal for IRI and truncated normal for
33 waviness number) as well as the non-parametric empirical PDF illustrated in Figure 4(b) for vehicle
34 speed. A total number of 100,000 samples are generated for Monte-Carlo simulations with their
35 estimated PDF also illustrated in Figure 3 and 4 by dashed lines. The probability distribution of excess
36 fuel consumption obtained from the Monte-Carlo simulation is presented in Figure 5 for both AC and
37 PCC pavements.

38 The results of the Monte-Carlo simulations are used to estimate the sensitivity of roughness-
39 induced excess fuel consumption to input parameter. Figure 6(a) and (b) show the SRCC between
40 roughness-induced excess fuel consumption and three input parameters (IRI, waviness number w , and
41 vehicle speed) for AC and PCC pavements. Positive and negative values of SRCC respectively indicate
42 direct and inverse relationship between input parameters and model outputs. For instance, increasing
43 IRI and reducing the waviness number result in an increase in excess fuel consumption. To compare the

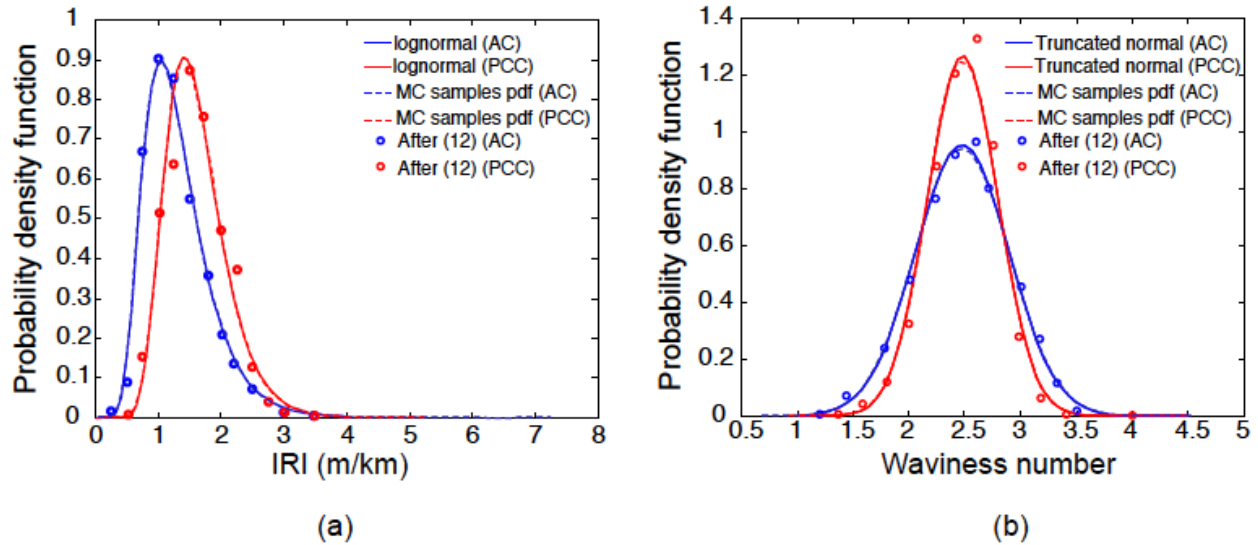
1 sensitivity of different input parameters, normalized SRCC is illustrated in Figures 6(c) and (d). The SRCC
 2 values, their 95% confidence bound and their normalized value are also summarized in Table 3. The
 3 sensitivity analysis reveals that roughness-induced excess fuel consumption is less sensitive to variation
 4 of vehicle speed, while both IRI and waviness number contribute significantly to the sensitivity of excess
 5 fuel consumption. This is not surprising: energy dissipation scales with $E[\delta\mathcal{E}] \sim V^{w-2}$, so that the impact
 6 of speed for the given distribution of waviness number (Fig. 3(b), Tab. 2) is minimized. In return,
 7 according to Eq. (9), energy dissipation scales with $E[\delta\mathcal{E}] \sim E[IRI]^2$, which explains the sensitivity of the
 8 model output w.r.t. variations in IRI. Finally, the sensitivity of the output w.r.t. the waviness number
 9 stems from both the velocity term and the amplification of the frequency response function in Eq. (9).
 10 The sensitivity of the model response to both IRI and w highlights the importance of two roughness
 11 parameters for an accurate determination of roughness-induced excess fuel consumption.

12

13 **Table 2 Mean and Standard Deviation for IRI and Waviness Number Adapted from Kropac and Mucka**
 14 **(12)**

Pavement type	Statistic	IRI [mm/m]	w [1]
AC	MEAN	1.320	2.475
	STD	0.541	0.417
PCC	MEAN	1.617	2.479
	STD	0.492	0.314

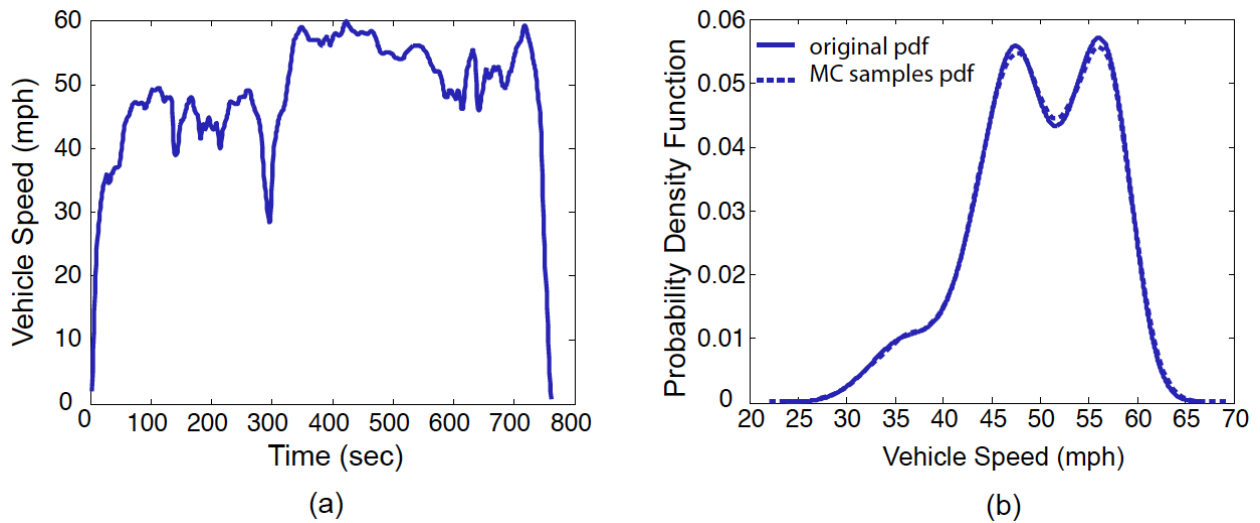
15



16

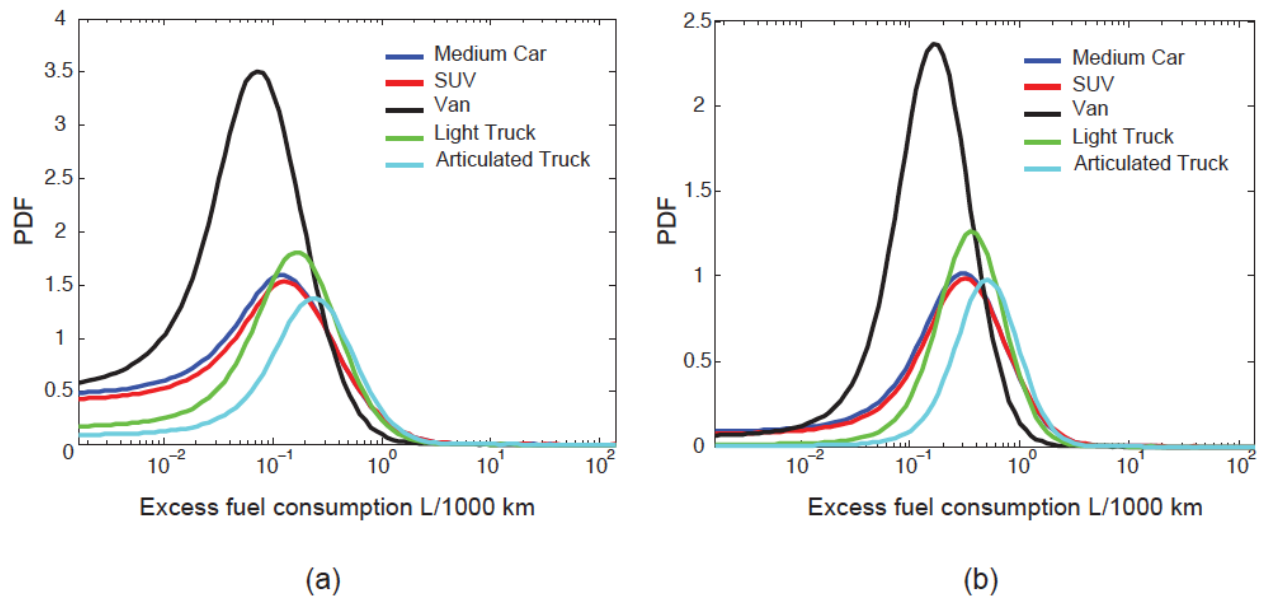
17 **FIGURE 3 Probability distribution function for (a): IRI; (b): waviness number. Dashed lines are the PDF**
 18 **of generated samples for Monte-Carlo simulation.**

19



1 **FIGURE 4** Vehicle speed (a): time history from the Highway Fuel Economy Driving Schedule (HWFED)
 2 provide by the US EPA (14); (b): probability density function evaluated from HWFED and by filtering
 3 out stop and go segments. Dashed lines are the PDF of generated samples for Monte-Carlo simulation.

4
5

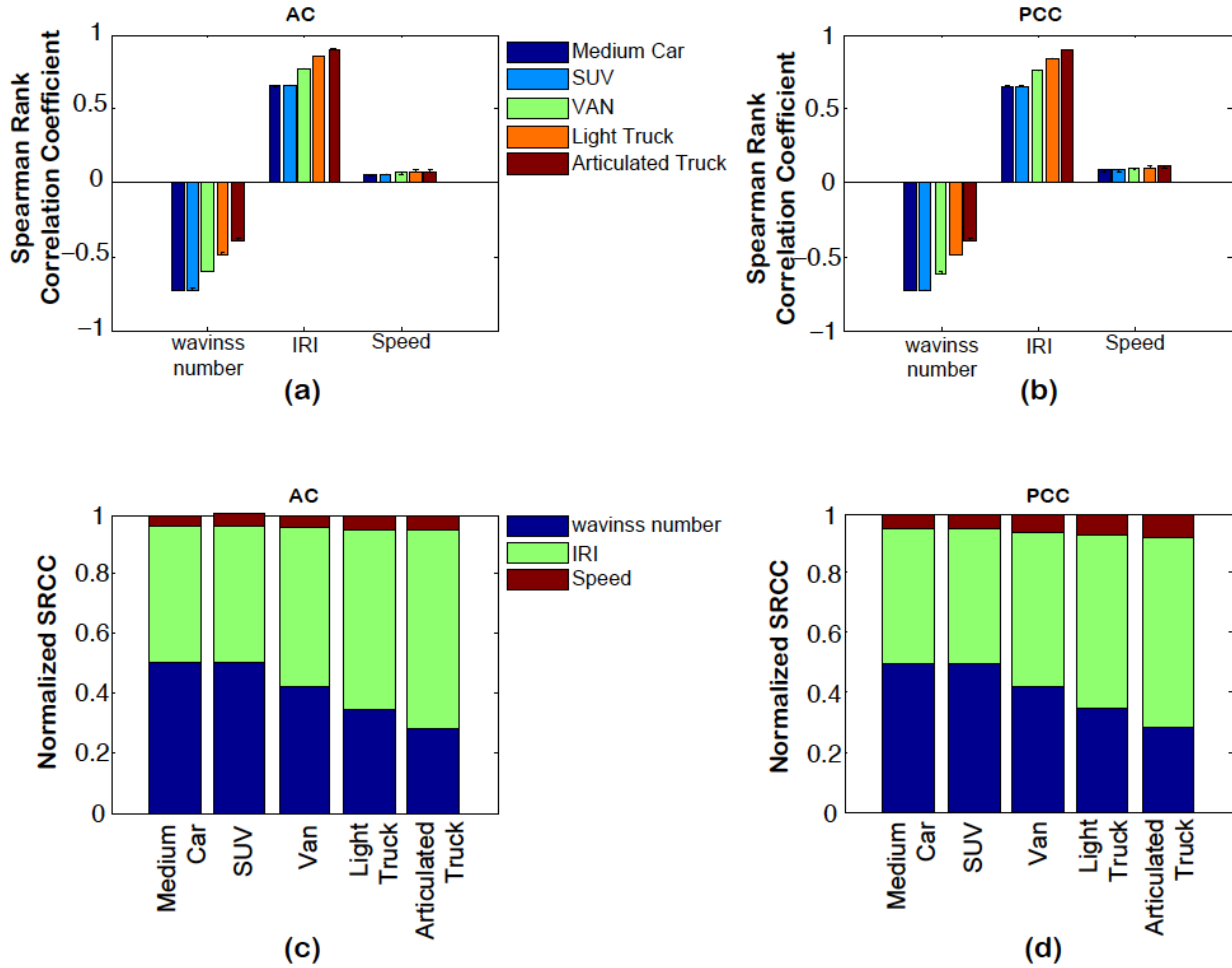


6 (a) (b)
 7 **FIGURE 5** Probability distribution of roughness-induced excess fuel consumption for five vehicle
 8 classes and for (a): AC pavements; (b): PCC pavements

9
10
11

1 **TABLE 3 Spearman Rank Correlation Coefficient with 95% Confidence Interval**

Pavement Type	cars	SRCC			Normalized SRCC %		
		Waviness number	IRI	Speed	Waviness number	IRI	Speed
AC	Medium Car	-0.7243 (-0.7273, -0.7214)	0.6522 (0.6486, 0.6557)	0.0547 (0.0485, 0.0609)	50.61	45.57	3.82
	SUV	-0.7231 (-0.7260, -0.7201)	0.6543 (0.6508, 0.6579)	0.0558 (0.0496, 0.0619)	50.46	45.65	3.89
	VAN	-0.6034 (-0.6073, -0.5994)	0.7664 (0.7638, 0.7690)	0.0645 (0.0584, 0.0707)	42.07	53.43	4.50
	Light Truck	-0.4849 (-0.4897, -0.4802)	0.8492 (0.8474, 0.8509)	0.0712 (0.0650, 0.0773)	34.51	60.43	5.07
	Articulated Truck	-0.3869 (-0.3922, -0.3816)	0.9017 (0.9005, 0.9029)	0.0755 (0.0693, 0.0816)	28.36	66.10	5.53
PCC	Medium Car	-0.7246 (-0.7276, -0.7217)	0.6495 (0.6460, 0.6531)	0.0796 (0.0735, 0.0858)	49.85	44.68	5.48
	SUV	-0.7254 (-0.7283, -0.7225)	0.6494 (0.6458, 0.6530)	0.0803 (0.0741, 0.0864)	49.85	44.63	5.52
	VAN	-0.6093 (-0.6132, -0.6054)	0.7587 (0.7561, 0.7613)	0.0920 (0.0858, 0.0981)	41.73	51.97	6.30
	Light Truck	-0.4889 (-0.4936, -0.4842)	0.8442 (0.8424, 0.8460)	0.1010 (0.0949, 0.1072)	34.09	58.87	7.04
	Articulated Truck	-0.3887 (-0.3939, -0.3834)	0.8985 (0.8973, 0.8997)	0.1066 (0.1005, 0.1128)	27.89	64.46	7.65



1
 2 **FIGURE 6** Plots of sensitivity of excess fuel consumption to different input parameters. Spearman
 3 rank correlation coefficients ρ evaluated for five vehicle classes used in calibrated HDM4 model for
 4 (a): AC pavements and (b): PCC pavements. Normalized SRCC as measure of sensitivity for (c): AC
 5 pavements and (d): PCC pavements.

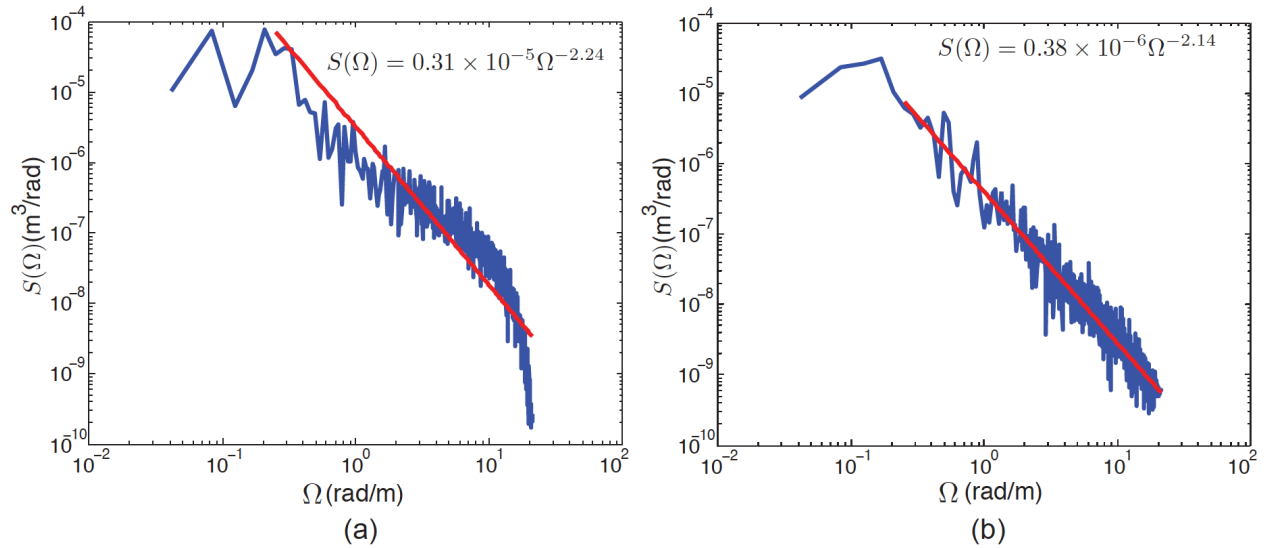
6
 7 **APPLICATION OF CALIBRATED ROUGHNESS MODEL WITH LTPP PROFILE DATA**

8 For purpose of illustration, we show how the mechanistic model can be employed when profile data is
 9 available. The profile data originate from FHWA’s Long-Term Pavement Performance (LTPP) program
 10 (15), in form of longitudinal profiles along the wheel path for in-service pavements measured over time
 11 to evaluate road roughness and its variations. The specific two sections employed are representative of
 12 two sections in California (06-9049 and 06-3042).

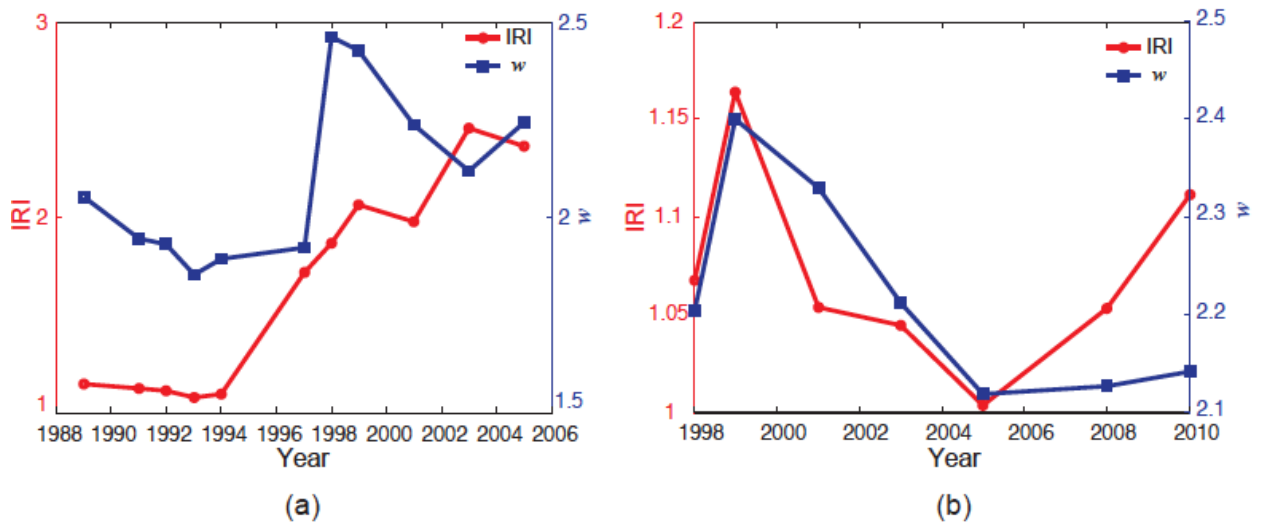
13 Employing the model with profile data requires in a first step the determination of the
 14 roughness PSD parameters. Assuming that road profiles are ergodic processes, this is achieved by
 15 performing a Fourier transformation of the profiles:

16
$$S_{\xi}(\Omega) = \lim_{x \rightarrow \infty} E \left[\left| \hat{\xi}(\Omega) \right|^2 \right] \tag{12}$$

1 where $(\hat{\cdot})$ denotes Fourier transform. The PSD parameters (c and w) are estimated by fitting a line to
 2 the PSD in log-log space (Figure 7). We also determine the IRI, and the average rectified slope for the
 3 golden car traveling with speed 80 km/h, for these profiles via the method described in Ref. (3). Figure 8
 4 shows the variation of IRI and waviness number over time for the two considered profiles.



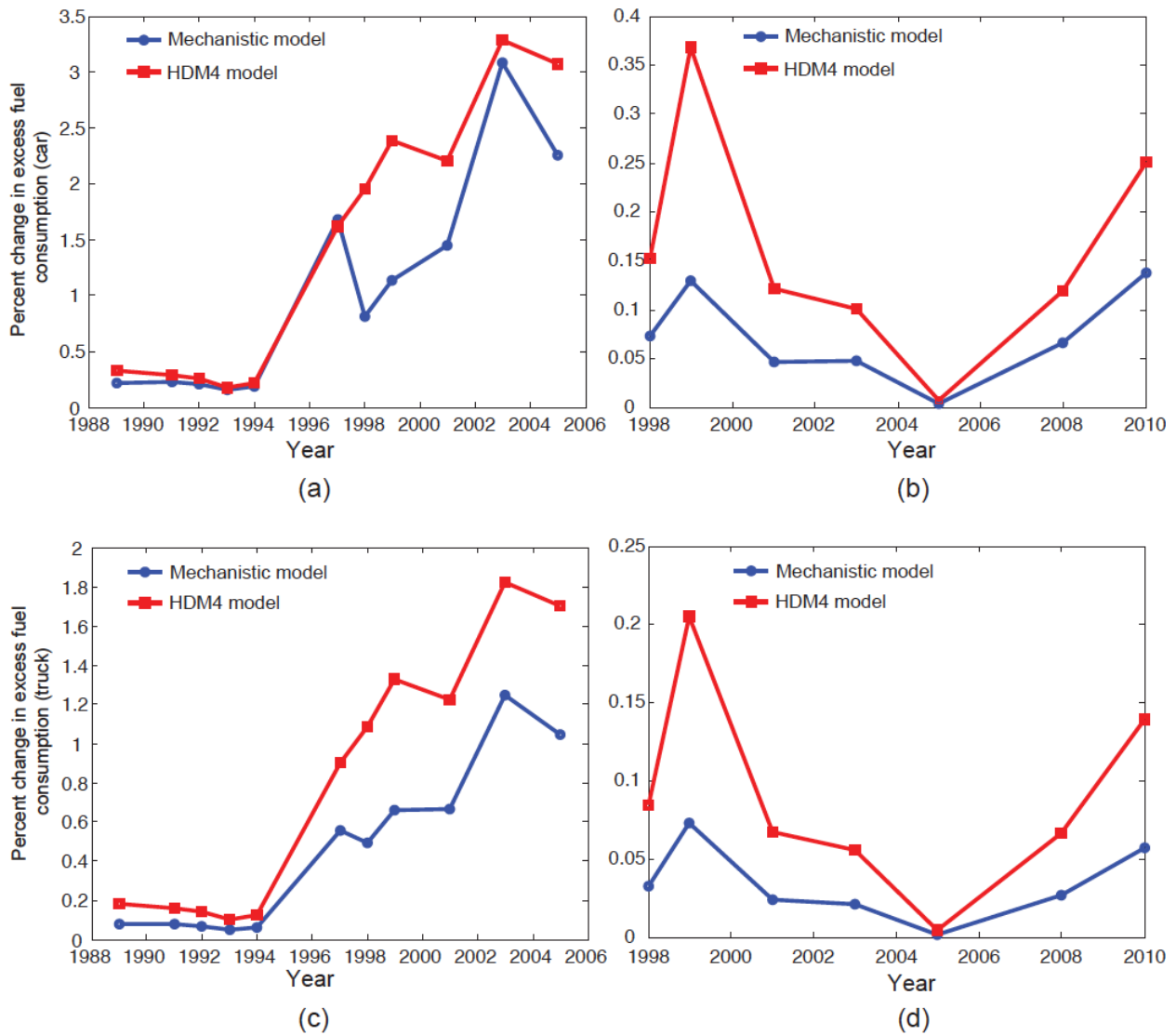
5
 6 **FIGURE 7** Plots of roughness power spectral density for (a): road profile of 06-9049 in 2010 and (b):
 7 road profile of 06-3042 in 2005 both located in California. Red line is the estimated power function
 8 for roughness PSD.



9
 10
 11 **FIGURE 8** Plots of IRI and waviness number over time for (a): road 06-9049 and (b): road 06-3042

12
 13 With the PSD parameters available, the excess fuel consumption due to pavement roughness is
 14 evaluated using both the mechanistic model as defined by Eqn. (9) and (10), and the HDM4 model. The

1 excess fuel consumption for a medium car and an articulated truck evaluated from the two methods are
 2 compared in Figure 9. Comparing the two LTPP sections in Figure 9, section 06-9049 has higher fuel
 3 consumption predicted by both methods than section 06-3042 mainly due to significantly higher IRI
 4 values. The excess fuel consumption obtained from the HDM4 model has the same trend as IRI. This is
 5 inevitable since this model uses only a single index, IRI, for road roughness representation. The
 6 mechanistic model results, however, do not exactly follow the variation of IRI, as the excess fuel
 7 consumption estimates depend on both IRI and waviness number w . It is also observed that for
 8 waviness numbers close to 2 the results from the two methods become very similar.



9
 10 **FIGURE 9** Plots of percent change in fuel consumption over time for (a): a medium car traveling on 06-
 11 9049; (b): a medium car traveling on 06-3042; (c): an articulated truck traveling on 06-9049 and (d): an
 12 articulated truck traveling on 06-3042

13

14 **CONCLUSIONS**

1 The mechanistic engineering model herein quantifies the impact of pavement surface characteristics on
2 vehicle fuel consumption as one source of energy dissipation related to Pavement Vehicle Interaction; in
3 addition to other sources of energy dissipation related to texture (16), and pavement structural and
4 material properties (17, 18). Such models are in high demand for evaluating the environmental footprint
5 of pavement structures during their use phase, contributing to the development of a quantitative
6 framework for pavement sustainable design and maintenance.

7 The distinguished feature of our model is that it combines a thermodynamic quantity (energy
8 dissipation) with results from random vibration theory in order to identify the governing parameters
9 that drive the excess fuel consumption due to pavement roughness:

- 10 1. While previous empirical approaches, like the HDM4 model (5,6), identified IRI as the key
11 engineering parameter driving roughness-induced excess fuel consumption, our results indicate
12 that (at least) a second road roughness parameter, namely the waviness number w , is required
13 to characterize the impact of pavement surface characteristics on vehicle energy dissipation and
14 fuel consumption. We come to this conclusion from a sensitivity analysis using Spearman rank
15 correlation coefficient method together with FHWA's LTPP database, which shows that the
16 predicted fuel consumption is as sensitive to the waviness number as it is to IRI. As shown in the
17 application of our model to two sections from LTPP database, this waviness number is readily
18 determined from profile data along with IRI.
- 19 2. In contrast to linear empirical relationships between IRI, rolling resistance and excess fuel
20 consumption proposed in the HDM4 model, our model forecasts a scaling of energy dissipation
21 with the square of IRI. This is due to the fact that the relative motion in a vehicle's suspension
22 system scales linearly with IRI, whereas the dissipated energy scales with the mean square of
23 suspension motion. That is, all other parameters equal, an increase of IRI by a factor of λ would
24 entail an increase of excess fuel consumption by a factor of λ^2 . This scaling is of some
25 importance for e.g. pavement management systems, which often use IRI as a metrics for
26 maintenance decisions.
- 27 3. In contrast to other sources of PVI-related excess fuel consumption, which show a high-
28 sensitivity to vehicle speed due to the viscoelastic nature of the pavement (17,18), we find that
29 roughness-induced excess fuel consumption is less sensitive to speed. This is due to the fact that
30 the energy dissipation scales with the speed as V^{w-2} , and that waviness numbers of pavements
31 are typically on the order of $w = 2.5 \pm 0.5$ (mean \pm standard deviation in LTPP database).
32 Otherwise said, a distinct speed sensitivity of PVI should not be attributed to roughness, but to
33 other sources of energy dissipation.

34 In summary, road roughness has been recognized to be a main contributor to vehicle rolling
35 resistance. It is thus necessary to come up with accurate roughness models for vehicle fuel
36 consumption. In this regard, introducing the waviness number, as a second roughness index, in addition
37 to IRI, allows a more accurate quantification of the impact of surface characteristics on vehicle fuel
38 consumption and the corresponding greenhouse gas emission. The new roughness index can be easily
39 evaluated by adding a module to the ProVAL software for implementation purposes.

40

41 **ACKNOWLEDGMENT:** This research was carried out by the CSHub@MIT with sponsorship provided by
42 the Portland Cement Association (PCA) and the Ready Mixed Concrete (RMC) Research & Education
43 Foundation. The CSHub@MIT is solely responsible for content.

1

2

3 **REFERENCES**

- 4 1. Velinsky, S.A., and R.A. White. Increased Vehicle Energy Dissipation Due to Changes in Road
5 Roughness with Emphasis on Rolling Losses. *SAE Technical Paper*, No. 790653, 1979, pp. 1-11.
- 6 2. Lu, X., Effects of road roughness on vehicular rolling resistance. *ASTM special Technical Publication*,
7 No 884, Edited by T.D. Gillespie and M. Sayers, Philadelphia, 1985, pp. 143-161.
- 8 3. Sayers, M.W. On the calculation of international roughness index from longitudinal road profile. In
9 *Transportation Research Record: Journal of the Transportation Research Board*, No. 1501,
10 Transportation Research Board of the National Academies, Washington, D.C., 1995, pp. 1-12.
- 11 4. Sayers, M.W., and S. M. Karamihas. The little book of profiling." *Ann Arbor: Transportation Research*
12 *Institute, University of Michigan*. <http://www.umtri.umich.edu/content/LittleBook98R.pdf>. Accessed
13 2014.
- 14 5. Chatti, K., and I. Zaabar. *Estimating the effects of pavement condition on vehicle operating costs*.
15 NCHRP Report 720. Transportation Research Board of the National Academies, Washington, D.C.,
16 2012.
- 17 6. Zaabar, I., and K. Chatti. Calibration of HDM4 Models for Estimating the Effect of Pavement
18 Roughness on Fuel Consumption for U.S. Conditions. In *Transportation Research Record: Journal of*
19 *the Transportation Research Board*, No. 2155, Transportation Research Board of the National
20 Academies, Washington, D.C., 2010, pp. 105–116.
- 21 7. Wang, T., I.S. Lee, A. Kendall, J. Harvey, E.B. Lee, and C. Kim. Life cycle energy consumption and GHG
22 emission from pavement rehabilitation with different rolling resistance. *Journal of Cleaner*
23 *Production* Vol. 33, 2012, pp. 86-96.
- 24 8. Sayers, M.W., T.D. Gillespie, and A.V. Queiroz. *The international road roughness experiment*.
25 *Establishing correlation and a calibration standard for measurements*. World Bank Tech. Paper No.
26 45, 1986, World Bank, Washington, D.C.
- 27 9. Dodds, C. J., and J.D. Robson. The description of road surface roughness. *Journal of Sound and*
28 *Vibration* Vol. 31, No. 2, 1973, pp. 175-183.
- 29 10. Robson, J. D. Road surface description and vehicle response. *International Journal of Vehicle Design*
30 Vol. 1, No. 1, 1979, pp. 25-35.
- 31 11. Johannesson, P., and I. Rychlik. Modeling of road profiles using roughness indicators. Accepted for
32 publication in *International Journal of Vehicle Design*, 2013.
- 33 12. Kropac, O., and P., Mucka. Indicators of longitudinal unevenness of roads in the USA. *International*
34 *journal of vehicle design*, Vol. 46, No. 4, 2008, pp. 393-415.
- 35 13. Spearman, C. The proof and measurement of association between two things. *American journal of*
36 *Psychology*, Vol. 15, No. 1, 1904, pp. 72-101.
- 37 14. United States Environmental Protection Agency, EPA Vehicle Chassis Dynamometer Driving
38 Schedules (DDS), <http://www.epa.gov/nvfel/testing/dynamometer.htm>, Accessed 2014.
- 39 15. FHWA, U.S. Department of Transportation. *LTPP: Long-Term Pavement Performance Program*.
40 <http://www.fhwa.dot.gov/research/tfhrc/programs/infrastructure/pavements/ltp>. Accessed 2014.
- 41 16. Sandberg, U., A. Bergiers, J.A. Ejsmont, L. Goubert, R. Karlsson, and M. Zöller. Road surface influence
42 on tyre/road rolling resistance. *Swedish Road and Transport Research Institute (VTI)*. Prepared as
43 part of the project MIRIAM, *Models for rolling resistance In Road Infrastructure Asset Management*
44 *systems*, 2011.
- 45 17. Louhghalam, A., M. Akbarian, and F-J Ulm. Flügge's Conjecture: Dissipation-versus Deflection-
46 Induced Pavement–Vehicle Interactions. *Journal of Engineering Mechanics*, Vol. 140, No. 8, 2013.

- 1 18. Louhghalam, A., M. Akbarian, and F-J Ulm. Scaling relations of dissipation-induced pavement-vehicle
2 interactions. In *Transportation Research Record: Journal of the Transportation Research Board*, No.
3 *14-0377*, Transportation Research Board of the National Academies, Washington, D.C., 2014.
- 4 19. Dixon, J. C. *Tires, suspension and handling*, Society of Automotive Engineers, Inc., Second edition,
5 1996.
- 6 20. Winkler, C. B. Evaluation of barrier limit capacity for different classes of vehicles and impact
7 conditions-parameter measurements of: 1978 Honda Civic, 1979 Dodge B-200 Van, 1979 Ford F150
8 Pickup. *Interim report*, No. *UMTRI-83-20*, 1983.
- 9 21. Fancher, P.S., R.D. Ervin, C.B. Winkler, and T.D. Gillespie. *A factbook of the mechanical properties of*
10 *the components for single unit and articulated heavy trucks*. No. *UMTRI-86-12*. 1986